Comparison of Survey Results of the Surface Quarry Spišské Tomášovce by the Use of Photogrammetry and Terrestrial Laser Scanning

Katarína PUKANSKÁ [1], Karol BARTOŠ [2], Janka SABOVÁ [3]

[1] Ing., Ph.D.; Institute of Geodesy, Cartography and Geographic Information Systems, FBERG, Faculty of Mining, Ecology, Process Control and Geotechnology, TUKE – Technical University of Košice, Park Komenského 19, 040 01 Košice, Slovak Republic; e-mail: katarina.pukanska@tuke.sk, tel.: +421 55 602 2978

[2] Ing.; Institute of Geodesy, Cartography and Geographic Information Systems, FBERG, Faculty of Mining, Ecology, Process Control and Geotechnology, TUKE – Technical University of Košice, Park Komenského 19, 040 01 Košice, Slovak Republic; e-mail: karol.bartos@tuke.sk

[3] Prof. Dr. Ing.; Institute of Geodesy, Cartography and Geographic Information Systems, FBERG, Faculty of Mining, Ecology, Process Control and Geotechnology, TUKE – Technical University of Košice, Park Komenského 19, 040 01 Košice, Slovak Republic; e-mail: janka.sabova@tuke.sk, tel.: +421 55 602 2976

Summary

In the area of spatial survey and modelling of irregular shapes of Earth's surface and complex structures, non-contact survey technologies are currently widely used. At present, terrestrial laser scanning, Lidar and terrestrial or aerial photogrammetry maintain probably the most important role within fast, accurate and mainly safe methods for obtaining information about the Earth's surface. The survey of surface quarry designed to quarrying wall stone – limestone was realized in the spring of 2013 by the use of terrestrial laser scanning and digital close-range photogrammetry, in order to determine exact geometrical shape of mined rock, together with subsequent survey in successive phases and calculation of the mined volume.

Keywords: surface quarry Spišské Tomášovce

Introduction

Terrestrial remote sensing techniques are being increasingly used as a complement to the traditional scanline and window mapping methods. They provide more comprehensive information on rock cuts, allow surveying of inaccessible outcrops, and increase user safety [5]. Non-contact survey technologies – such as terrestrial laser scanning and digital close-range photogrammetry, have a unique place in the area of surveying techniques of unstable rock formations, sub-soil, quarries and geological structures. Their benefits are:

- rapid acquisition of 3D information about complex shaped objects – time saving,
- measurement of inaccessible or dangerous places,
- cost-effective methods in comparison with time and processing demands.

Digital close-range photogrammetry can be characterized by imaging distance $h <$ ca. 300m [2], which is fully sufficient for the survey of our place of interest. In contrast to the analytical photogrammetry, which has undergone earlier historical development during the last century, laser scanning – and especially terrestrial laser scanning, is the major mapping technology of the past decade. Its application is mainly in architecture, civil engineering, engineering surveying, geology, but also in related fiel

Methodology of the survey

On the basis of statutory regulation of the *Act No. 44/1988 on the protection and use of mineral resources* (*The Mining Act*), § 10 par. 1 b) and c), the organization performing mining activities is obliged to:

- a) manage the mining-surveying and geological documentation,
- b) register the stock level of exclusive deposit and its changes.

In cooperation with the owner of the quarry, we decided to realize survey of the surface quarry of limestone by the use of two already mentioned technologies – terrestrial laser scanning using *Leica ScanStation C10* (Fig. 3) and digital close-range photogrammetry using digital SLR camera *Canon 50D* and wide-angle lens *Canon EF 20mm/f2,8 USM*. The quarry is situated in the eastern part of Slovakia, near the National Park Slovak Paradise (Fig. 1).

Terrestrial laser scanning

The spatial position of individual points measured by terrestrial laser scanner *Leica ScanStation C10* is determined in local coordinate system [9], with the origin at the center of the scanner (Fig. 2). These coordinates are calculated using equations (1, 2, 3), where d is slope distance, ω is horizontal angle and ζ is zenith angle. *Leica ScanStation C10* is

Fig. 1. Map of locality of the surface quarry Spišské Tomášovce

Rys. 1. Mapa lokalizacji kamieniołomu Spišské Tomášovce

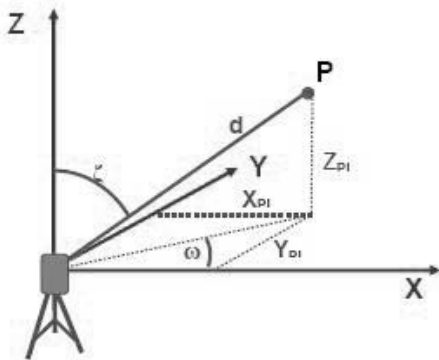a full panoramic long-range pulse scanner with an accuracy of 6 mm in position and 4 mm in length (Fig. 3, Tab. 1).

Fig. 3. TLS Leica ScanStation C10

Rys. 3. Skaner TLS Leica ScanStation C10

Fig. 2. The principle of spatial polar method [2, 6]

Rys. 2. Zsada metody polaryzacji powierzchniowej [2, 6]

$$x = d \cdot \cos(\omega) \cdot \sin(\zeta) \qquad (1)$$

$$y = d \cdot \sin(\omega) \cdot \sin(\zeta) \qquad (2)$$

$$z = d \cdot \cos(\zeta) \qquad (3)$$

Five survey stations were monumented in the area of quarry after the terrain reconnaissance. Spatial position of these stations was determined in the local coordinate system by the use of robotic total station *Trimble VX Spatial Station*® (Fig. 4), characterized with range up to 800 m and accuracy of 1 mm + 2 ppm in length with surveying prism.

Tab. 1: Technical specification of the Leica ScanStation C1

Tabela 1. Specyfikacja techniczna skanera Leica ScanStation C1

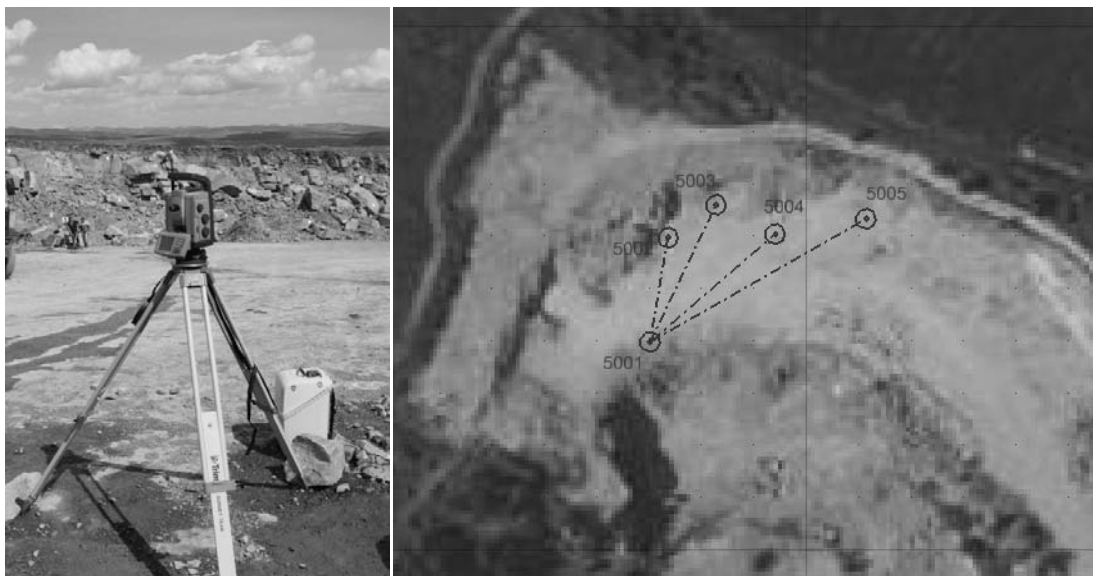| Technical specification of the laser scanner	
Accuracy of single measurement	
Position/Distance	6 mm/4 mm
Angle precision	
Horizontal/Vertical	12'' / 12''
Modeled surface precision	2 mm
Range	300 m @ 90%; 134 m @ 18%
Minimal step of scanning	1 mm
Scan rate	50 000/sec.
Laser class	3R, green (λ = 532 nm)
Spot size	0-50 m ≈ 4,5 mm
Field of view	
Vertical/Horizontal	270°/360°

Fig. 4. Trimble VX Spatial Station® and general overview of the quarry

Rys. 4. Trimble VX Spatial Station® i widok ogólny kopalni

Real measurement errors ε can be determined on the basis of following terms (see frame at the bottom of this page) [2, 6].

As a part of the survey, the quarry wall was scanned from a distance of about 20 m, with a grid density of 2 × 2 cm, resulting in a 1,5 million points. The disadvantage of *Leica ScanStation C10* is integrated digital camera with low geometric and radiometric resolution, which not only reduces a presentation value of the result, but also its correct representation. The scanned surface had a suitable color texture for a quality record of scanning – it was dry, with bright color and rough structure, without smooth and shiny surfaces.

Optical (photogrammetric) scanning

Photogrammetric scanner is a relative innovation in photogrammetry, although it has been used in aerial photogrammetry for several years. The accuracy and method of imaging is based on the principle of stereophotogrammetry, but the method of evaluation is fundamentally different. It is based on the principle of image correlation, where the image points (pixels) are measured automatically. Therefore the photogrammetric scanner becomes extremely effective tool. Practically, malfunction in the case of objects without texture or more noise on the objects with less significant texture is disadvantage.

Digital image correlation

The current technology of automatic digital processing of photogrammetric images often uses the principle of image correlation of two sub-images. The aim is to find the position of two corresponding (homologous) points without intervention of operator and get their image coordinates. Further processing depends on the main objective of processing. The principle of digital image correlation is based on comparing two images among themselves and finding a pair that is the most similar. For the purpose of objective assessment of the similarity between images, it is necessary to define some similarity measure. The coefficient of selective correlation (correlation coefficient) is the most commonly used:

$$\rho(A,B) = \frac{\text{cov}(A,B)}{\rho(A) \cdot \rho(B)} \tag{7}$$

where: cov*(A, B)* is a covariance and $\rho(A)$ and $\rho(B)$ are mean errors and their roots are variances. To compute the correlation coefficient for two digital images (or their cut-outs) of the same size, we can use the pixel value $p(A)_{i,j}$ for the image A and $p(B)_{i,j}$ for the image B. Then we get following relation:

$$r(A,B) = \frac{C(A,B)}{\sqrt{C(A) \cdot C(B)}} \tag{8}$$

$$\varepsilon_x = \cos(\omega) * \sin(\varsigma) * \varepsilon_d - d * \sin(\omega) * \sin(\varsigma) * \varepsilon_\omega + d * \cos(\omega) * \cos(\varsigma) * \varepsilon_\varsigma \tag{4}$$

$$\varepsilon_y = \sin(\omega) * \sin(\varsigma) * \varepsilon_d + d * \cos(\omega) * \sin(\varsigma) * \varepsilon_x + d * \sin(\omega) * \cos(\varsigma) * \varepsilon_\varsigma \tag{5}$$

$$\varepsilon_z = \cos(x) * \varepsilon_d - d * \sin\cos(\varsigma) * \varepsilon_\varsigma \tag{6}$$

$$C(A,B) = \frac{1}{n^2 - 1} \sum_{i=1}^{n} \sum_{j=1}^{n} \left(p(A)_{i,j} - \overline{p}(A) \cdot \left(p(B)_{i,j} - \overline{p}(B) \right) \right)$$

$$C(A) = \frac{1}{n^2 - 1} \sum_{i=1}^{n} \sum_{j=1}^{n} \left(p(A)_{i,j} - \overline{p}(A) \right)^2 \ , \quad \overline{p}(A) = \frac{1}{n^2} \sum_{i=1}^{n} \sum_{j=1}^{n} \left(p(A)_{i,j} \right)$$ (9)

$$C(B) = \frac{1}{n^2 - 1} \sum_{i=1}^{n} \sum_{j=1}^{n} \left(p(B)_{i,j} - \overline{p}(B) \right)^2 \ , \quad \overline{p}(B) = \frac{1}{n^2} \sum_{i=1}^{n} \sum_{j=1}^{n} \left(p(B)_{i,j} \right)$$

where individual terms are represented by the formulas 9 (n is the number of pixels in the side of the square window) [7].

Technique of searching points

Coordinates of some important objects can be determined automatically. The method used is to search of objects on the basis of correlation. Points in an image can be found automatically while respecting certain conditions. There are two methods:

- we know how the object look like and we are able to create its model shape,
- we have a general point in one image (e.g. from a stereo pair) and we are looking for homologous point in the second image.

For both types, we have to select a sufficient surrounding of object or point in the form of image sub-matrix (sample window). In the known or estimated approximate position of the searched object, we can select a sufficiently large search area (again a sub-matrix), in which we select the search window with the same size as the sample window. We can calculate their mutual image correlation (correlation coefficient) and determine the position of center of the search window in image, then we move the search window in the search area by one pixel and we again calculate the correlation coefficient and again determine the position of center of the search window. This way, we can go with the search window through the whole search area. Assuming that the search and image window have N × N pixels and search area has M × M pixels (where M > N), we obtain total of $(M - N + 1)^2$ correlation coefficients. The position of pixel with the maximum value of the correlation coefficient r is the center of the search object or the searched point [7].

Processing of the measurement results

1 longitudinal section and 4 cross sections were made at almost vertical locations of walls of the quarry (Fig. 8), for analysis of the surface processed by different technologies. 37 ground control points in the form of 12-bit coded targets was stabilized in the terrain (distributed according to the Fig. 6) for the purposes of digital photogrammetry. The spatial position of these points was determined by electronic total station. The imaging distance does not exceed 20 m, when we can achieve the precision abreast of laser scanning [1]. 16 stereo image pairs were acquired on the basis of stereophotogrammetric imaging, which were processed by the algorithm of digital image correlation and subsequently the final point cloud and mesh model of the whole quarry surface were generated (Fig. 9). The final point cloud contains 3.491 mil. of reconstructed points. In photogrammetric processing, the following accuracy was achieved – unit mean error of 0.39, *a posteriori* accuracy of 0.332 pix, maximum residual of 1.948 pix and overall RMS vector length of 7.5 mm.
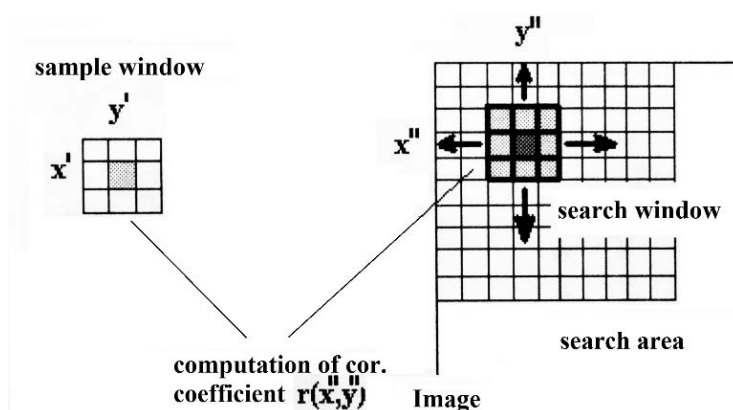

Fig. 5. Correlation of image windows.[7]
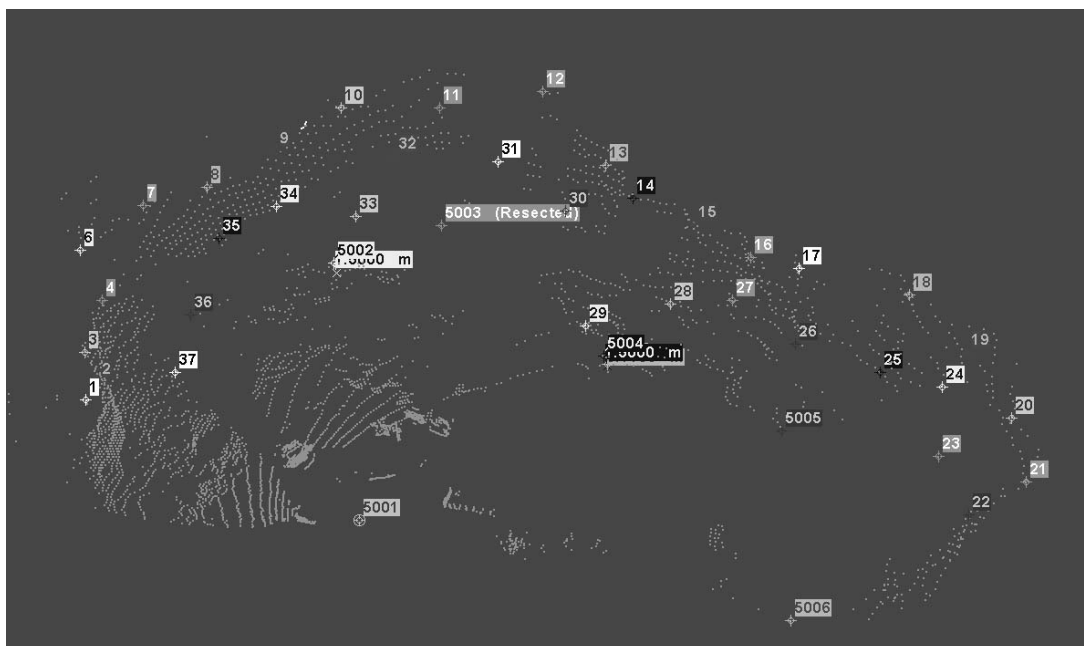
Rys. 5. Korelacja okien obrazu

Fig. 6. General overview of deployment of the ground control points on the quarry surface

Rys. 6. Schemat ogólny rozmieszczenia naziemnych punktów kontrolnych na powierzchni kamieniołomu
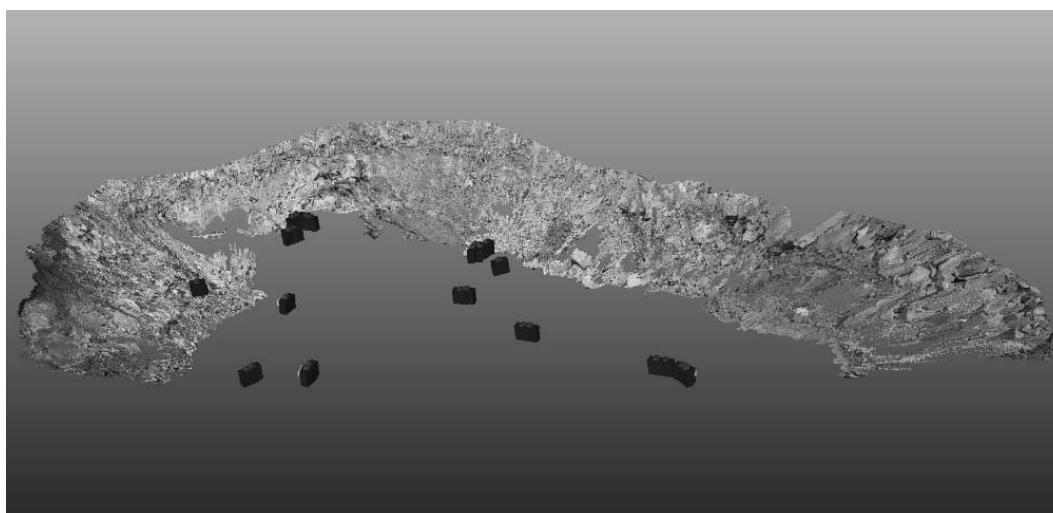

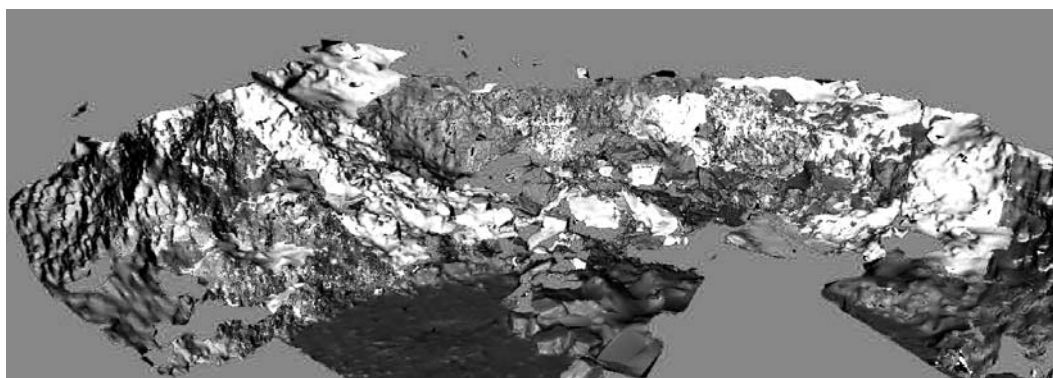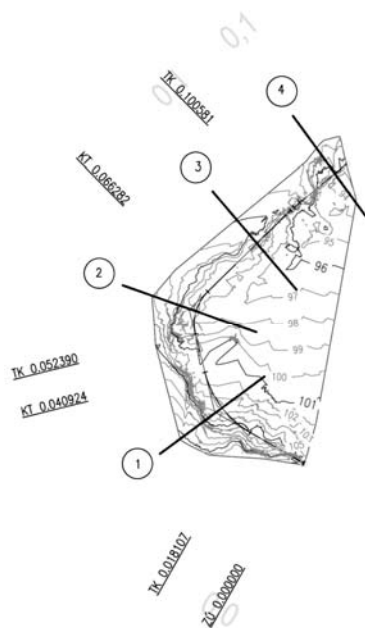Fig. 7. Camera configuration

Rys. 7. Konfiguracja aparatu

Fig. 8. Identified TIN surfaces (white color – surface from photogrammetry; grey – laser scanning)

Rys. 8. Identyfikacja powierzchni TIN (kolor biały – nawierzchnia z fotogrametrii; szary – skanowanie laserowe)

longitudinal profile: 4 M 1:1/1
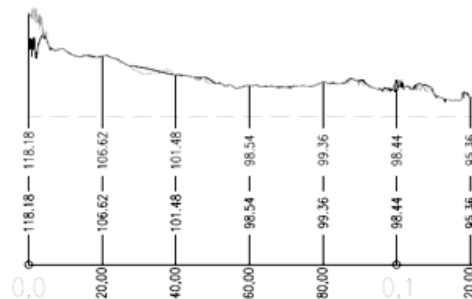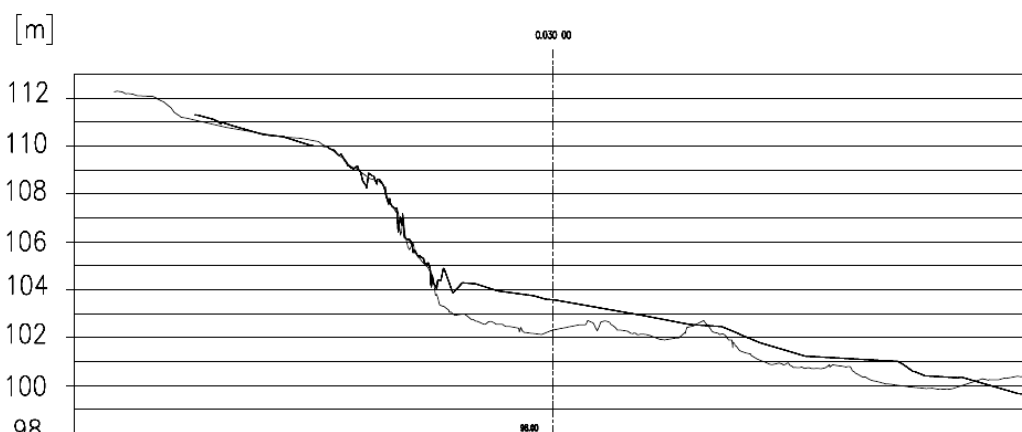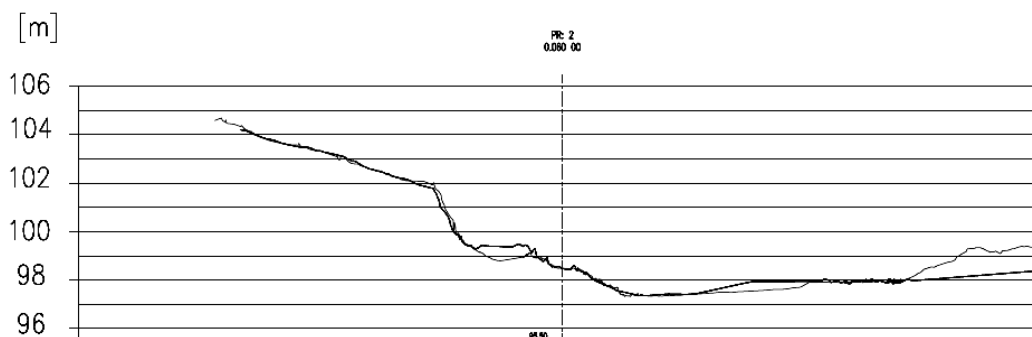range: km 0,00000 - km 0,12175

Fig. 9. General overview of the longitudinal
section and cross sections through the quarry

Rys. 9. Widok ogólny przekroju podłużnego
i przekrojów przez kamieniołom

Fig. 10: Longitudinal section through the quarry

Rys. 10. Przekrój podłużny przez kamieniołom

a) cross section No.1

b) cross section No.2

Fig. 11a. Cross sections a), b) – black from the laser scanning, grey from photogrammetry

Rys. 11a. Przekroje a), b) – czarny – ze skanowana laserowego, szary – z fotogrametrii
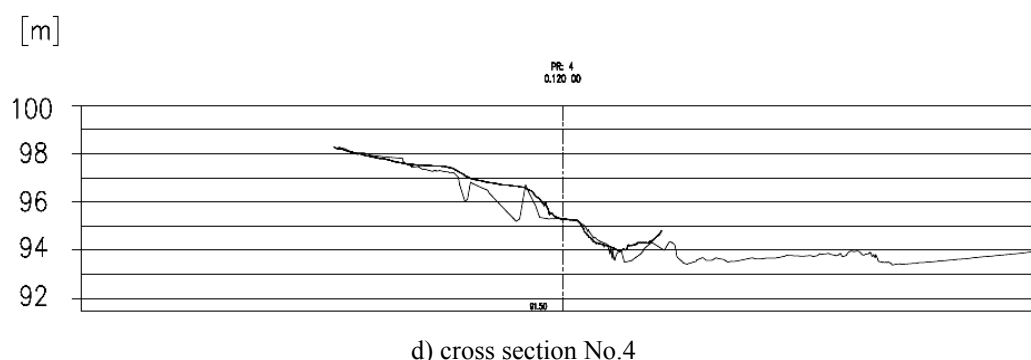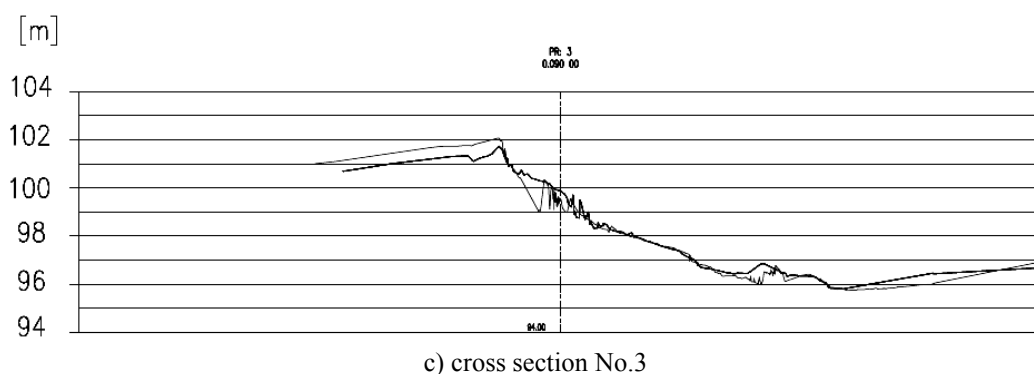
c) cross section No.3

d) cross section No.4

Fig. 11b. Cross sections c), d) – black from the laser scanning, grey from photogrammetry

Rys. 11b. Przekroje c), d) – czarny – ze skanowana laserowego, szary – z fotogrametrii

Conclusion

In conclusion we can say that despite the fact, that same type of data (point clouds) are inputs in processing of TIN models, both technologies are characterized by significant differences in their usage and processing of data acquired. Parts of quarry, in which the individual sections were generated (mainly in vertical parts of the quarry wall), were selected for surface analysis of both methods. Based on the visualization of cross sections we can see, that the biggest differences in modeled surface can be found in the cross section No. 1 in the area of the axis of longitudinal section, in slightly sloped terrain. Due to the fact that the laser beam is highly directional it can not to curve, whereby so-called holes occur in the scanned area and thereby it is not possible to get all details of the surface shapes. Similarly, surface details could not be obtained due to the occlusions in the cross section No. 4 to the left of the axis. Since it is relatively easier to select survey stations especially in photogrammetric scanning, so that we can get better recorded surface, the line of curve of sections through the photogrammetric TIN model are more detailed.

In practice, both technologies are suitable for this type of survey, but it is necessary to avoid occlusions and unwanted objects obscuring our object of survey when choosing individual survey stations, especially in terrestrial laser scanning, since they can cause a significant degradation in quality of result. The advantage of terrestrial photogrammetry is a greater variability in camera configuration, but also in this case there is a chance of occurrence of occlusions and obscuring objects, especially in the rugged terrain. For this reason, it would be ideal to use an aerial UAV technology navigated by GNSS, which are increasingly more accessible.

Literatura – References

1. Fraštia M.: Laser vz. optical scanning of rock massifs, Mineralia Slovaca, 44 (2012), 177–184, ISSN 1338-3523, http://www.geology.sk/doc/min_slov/ms_2012_2/MS_2_2012_07_Frastia_na%20web.pdf

2. Kraus K.: Photogrammetry, Vol. 2, pp. 466, Bonn 1997

3. Luhmann T., Robson S., Kyle S., Harley I.: *Close range photogrammetry: principles, methods and applications, Caithness, Whittles Publishing, 2006*

4. Pavelka K.: *Fotogrammetrie 3, Digital methods and laser scanning, CVUT, 2008, Prague*

5. Sturzenegger M., Stead, D.: *Close-range terrestrial digital photogrammetry and terrestrial laser scanning for discontinuity characterization on rock cuts, Engineering Geology, 106, 2009, p.163–182, ISSN: 0013-7952*

6. Štroner M., Pospíšil J.: *Terrestrial scanning systems (Terestrické skenovací systémy), Czech technical university in Prague (České vysoké učení technické), Praha 2008, ISBN 978-80-01-04141-3*

7. Pavelka K.: *Fotogrammetrie I. Praha, FSv, ČVUT, 2009, ISBN 978-80-01-04249-6*

8. Sabo J., Antoško M.: *Hybrid navigation techniques in aviation with using the GNSS. In: Acta Avionica. Roč. 14, č. 25 (2012), s. 90-92. - ISSN 1335-9479*

9. Weiss G., Gašinec J., Engel J., Labant S., Rákay Š. ml.: *Effect incorrect points of the Local Geodetic Network at results of the adjustment. In: Acta Montanistica Slovaca. Vol.13, No. 4 (2008), pp. 485-490. ISSN 1335-1788. http://actamont.tuke.sk/pdf/2008/n4/12weiss.pdf*

Porównanie wyników pomiaru powierzchni kamieniołomu Spišské Tomášovce za pomocą fotogrametrii i naziemnego skaningu laserowego

W dziedzinie badań i modelowania przestrzennego nieregularnych kształtów na powierzchni Ziemi oraz struktur kompleksowych technologie bezdotykowe znajdują szerokie zastosowanie. Obecnie naziemny skaning laserowy Lidar oraz naziemna i powietrzna fotogrametria pełnią prawdopodobnie najważniejszą rolę w związku z szybkim, dokładnym i bezpiecznym pomiarem dostarczającym informacji na temat powierzchni Ziemi. Pomiar powierzchni kamieniołomu wydobywającego wapienny kamień ścienny został przeprowadzony wiosną 2013 roku przy użyciu naziemnego skaningu laserowego oraz fotogrametrii cyfrowej bliskiego zasięgu w celu określenia dokładnego kształtu wydobywanego kamienia, a następnie obliczono ilość wydobywanego materiału.

Słowa kluczowe: kamieniołom Spišské Tomášovce